

Galaxies form at peaks—Not!

FERMILAB-Pub-92/237-A

Neal Katz¹, Thomas Quinn², and James M. Gelb^{1,3}

¹Department of Physics, M.I.T., 6-214, Cambridge, MA 02139

²Theoretical Physics, Keble Road, Oxford OX1 3NP

³NASA/Fermilab Astrophysics Center, P.O. Box 500, Batavia, IL 60510

SUMMARY

A large N -body simulation is used to compare the galaxies found by tagging peaks in the linear density field with the halos that actually form. A variety of filters on the density field are tried in order to improve this correspondence, but none seems to do particularly well. The correlation function and velocity dispersion of the tagged peaks and the actual halos also do not correspond very well. These comparisons bring into question the results of any study of galaxy formation that assumes that galaxies form at peaks in the initial density field or simulations of large scale structure that use the high peak model to determine the galaxy distribution.

1 INTRODUCTION

An outstanding problem in verifying cosmological models is the relationship between the mass distribution and the light distribution. Most modeling follows the evolution of the mass distribution, while observations are made of the light. The simplest method for connecting the two is to assume that the mass density is proportional to the luminosity density, i.e. that the mass traces the light. However, in the gravitational instability picture, this assumption has run into serious difficulties. For example, with the initial power spectrum predicted by the Cold Dark Matter (CDM) model, N -body simulations have shown that the correlation function of the matter steepens with time (Davis *et al.* 1985). When the slope of the correlation function is equal to the observed slope, the correlation length is $r_0 \approx 1.3h^{-2}$ Mpc for $\Omega = 1$, which would require a Hubble constant of $H_0 = 25 \text{ km s}^{-1}$ to match the observed correlation length of $r_0 \approx 5.4h^{-1}$ Mpc (Davis and Peebles 1983). This is much smaller than any observational estimates for H_0 . Also, the RMS peculiar velocities of the dark matter are $\sim 1000 \text{ km s}^{-1}$ in the numerical simulations; much higher than the observed value of $300 \pm 50 \text{ km s}^{-1}$ for galaxies. A simple method of relaxing the assumption that mass traces light is to make the hypothesis that galaxies preferentially form in higher density regions. With this assumption, the galaxy distribution forms a “biased” estimate of the mass distribution, and the correlation function of the galaxies is enhanced by a factor b^2 , where b is a “bias factor”, over that of the mass (Kaiser 1984, and Bardeen *et al.* 1986 (BBKS)). Due to

this enhancement in the correlation amplitude, the correlation length is able to match the observed value when the simulation is less evolved, thereby giving the correlation function a shallower slope and reducing the RMS peculiar velocities.

A common way to model galaxy bias is to assume that galaxies form only at high peaks in the initial density field, known as the high peak model for galaxy formation. Using the formalism of BBKS, one can derive many useful galaxy properties just by studying peaks in the initial density field. This assumption has also been used in many numerical simulations to identify galaxies (e.g. Davis *et al.* 1985). To simplify their analytic calculations, BBKS introduced the peak-background split to identify the sites of galaxy formation. The peak-background split makes use of the fact that the density of high peaks on a small scale (i.e. the scale of galaxies) can be estimated from the background density smoothed on a larger scale. For many properties concerning both the distribution and velocities of galaxies this technique yields results that are statistically similar to those obtained by actually following peak tracers (Park 1991). The peak-background split is particularly useful for studying the formation of large scale structure. Given the limited range of even the largest N -body simulations, it allows modeling of the galaxy distribution in simulations of large scale structure that do not have the resolution to determine the evolution of individual galaxies (White *et al.* 1987b, Weinberg and Gunn 1990, Park 1990, Park and Gott 1991). The peak-background split has also been applied to simulations of galaxy clus-



ters (Frenk *et al.* 1990, Dalton *et al.* 1992).

Various proposals have been put forward to provide a physical mechanism for biasing, such as gas-dynamical feedback mechanisms suppressing the formation of low mass galaxies (Dekel and Silk 1986). The possibility that biasing could occur “naturally”, *i.e.* through normal hierarchical clustering, has been discussed by Frenk *et al.* (1988) (FWDE). By studying N -body simulations of small regions of the universe (~ 14 Mpc) at high resolution, they showed that massive halos formed preferentially in regions of high density. This happens because the higher background density accelerates the formation of structure, including the formation of heavy halos, when compared to regions of average background density. However, their conclusions of how this affects large scale structure are somewhat limited due to the small size of their simulated regions.

Although Park (1991) has shown that the peak-background split is statistically equivalent to following high peak tracers, only FWDE attempted to determine if the high peak model correctly identifies the sites of galaxy formation. They conclude that the high peak model works quite well but their conclusion may have been compromised by the small size of their simulated regions. Also, they only modeled a low amplitude CDM spectrum and one might expect the correlation between high peaks in the initial density field and actual sites of galaxy formation to weaken as the simulations become more evolved.

Here, we aim to investigate how well the high peak model describes the sites of galaxy formation and the “natural biasing” that occurs in gravitational collapse models by studying a simulation that is both large enough to model the formation of large scale structure, and of high enough resolution to model the formation of individual halos. First the simulation used for this investigation is described, then the results are presented and discussed.

2 SIMULATION

To obtain the large dynamic range needed to follow the collapse of individual galaxies while correctly following the development of large scale structure, simulations with large numbers of particles and high resolution forces are needed. The simulation we use is described in detail in Gelb (1992) and contains 144^3 particles in a 5000 km s^{-1} box with periodic boundary conditions. The particles are evolved using a modified version of Couchman’s (1990) adaptive Particle-Particle-Particle-Mesh (PPPM) algorithm. Each particle has a mass of $2.324 \times 10^{10} M_{\odot}$, and the form of the force softening is a Plummer model with $\epsilon = 65$ kpc, constant in comoving coordinates.

The initial conditions are a realization of a Cold Dark Matter density distribution with $\Omega = 1.0$ and are pro-

duced by perturbing the particles off a cubic lattice using the Zel’dovich approximation. The power spectrum is that given by BBKS with the amplitude determined by setting the linearly extrapolated $\Delta M/M$ in $8h^{-1}$ Mpc spheres to 1. The simulation starts at an expansion factor of 1/70 where an expansion factor of 1.0 represents the present if there is no bias; the output is studied at expansion factors of 0.5, 0.7, and 1.0, corresponding to biases of 2.0, 1.43, and 1.0, respectively.

Peaks in the initial density field are found by first evaluating the density field on a 144^3 grid, then smoothing the density field with a given filter, and finally locating grid points that are higher than all 26 neighboring grid points. The evolution of these peaks are then followed by tagging the particles closest to the peak grid points, and examining the distribution of these tagged particles at later times.

Bound groups in the simulations are identified using the DENMAX algorithm described in Gelb (1992) and Bertschinger and Gelb (1991). This involves using the particle positions to evaluate the density on a very fine grid (512^3), and allowing the particles to follow the density gradient upward until they end up at a density peak. All the particles ending at a given peak are considered to be one group. These particles are then checked to see if they are gravitationally bound to the rest of the particles in the group, and discarded if they are not. We only consider those groups whose mean density within 150 comoving kiloparsecs is greater than 200 times the mean density. This ensures that the groups actually are collapsed objects. The density cutoff requires that the groups contain at least 9 particles—a mass of $2 \times 10^{11} M_{\odot}$.

3 RESULTS

The main concern of this paper is the correspondence between peaks in the linear density field and the groups (halos) that subsequently form out of that field. To this end we investigate whether particles tagged as belonging to peaks end up in groups, and therefore, how well these peak particles mimic the distribution of groups. At several times, corresponding to different biases, we examine all the peak particles to determine if they have become part of a group as defined above, and to determine if there is a correlation between the peak height and the group mass.

Figures 1 and 2 show the results for a Gaussian filter with two different smoothing radii and at the three different times. The two smoothing radii, $R_f = 0.55$ Mpc and 0.88 Mpc ($H_0 = 50 \text{ km s}^{-1} \text{ Mpc}^{-1}$), correspond to masses of $\sim 2 \times 10^{11} M_{\odot}$ and $\sim 8 \times 10^{11} M_{\odot}$. In Figures 1 and 2, the panels in the upper row use a filter mass of $2 \times 10^{11} M_{\odot}$ and the lower panels use $8 \times 10^{11} M_{\odot}$. The first column is at an expansion factor of 0.5, the second column is at 0.7, and the last column is at 1.0.

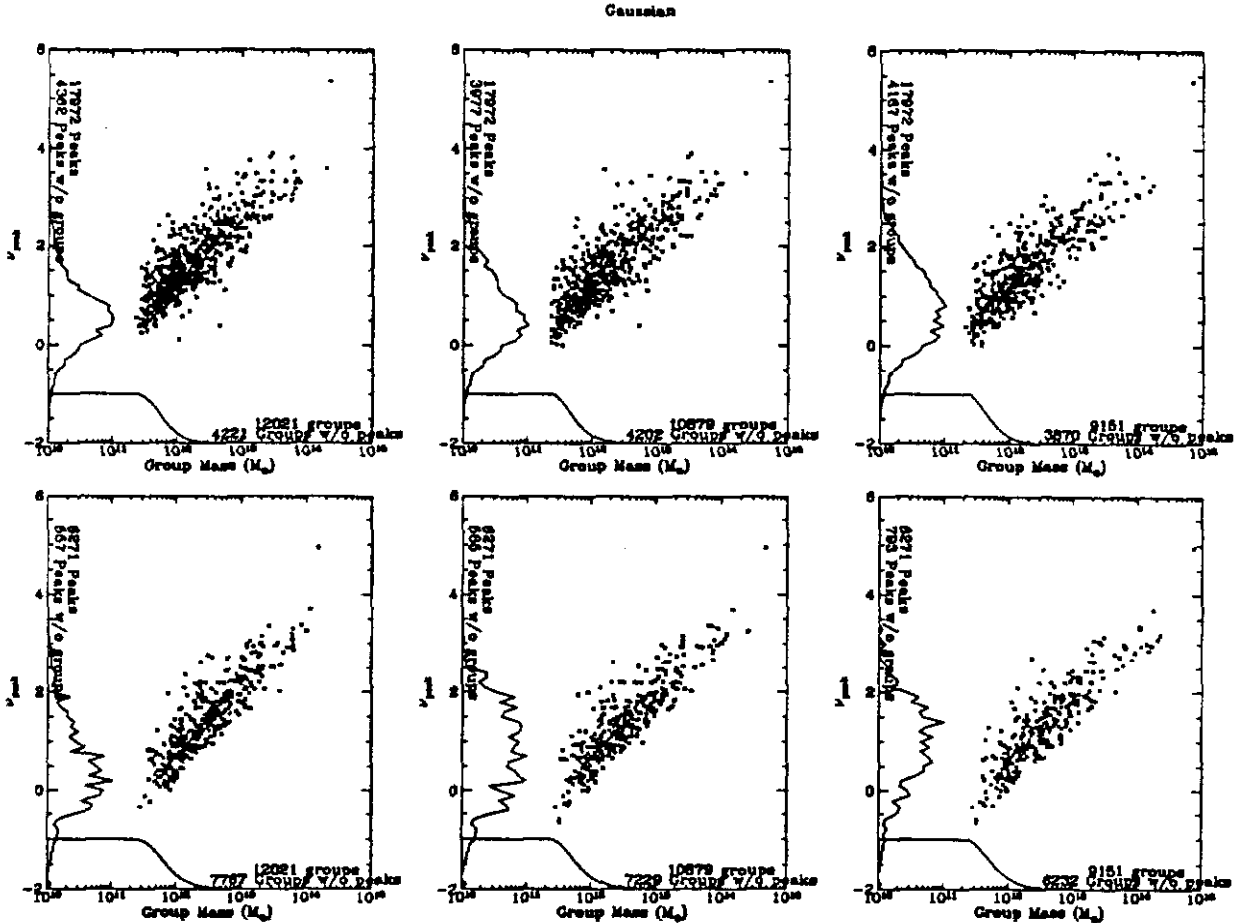


Figure 1. The peaks in the filtered initial density field that are associated with groups are plotted, showing the initial peak height against the group mass. The initial peak height is in units of the standard deviation of the linear density field. The highest peak associated with a group is indicated with a "x". To avoid crowding, only one out of every ten peaks is plotted. A Gaussian filter is used on the initial density field. The plots in the upper row are for a filter length of $R_f = 0.55$ Mpc, while the lower row is for $R_f = 0.88$ Mpc. The left column is for an expansion factor $\alpha = 0.5$, the middle for $\alpha = 0.7$, and the right for $\alpha = 1.0$. The line along the horizontal axis is the cumulative distribution in group mass of groups with no peak associated with them. The line along the vertical axis is the differential distribution in peak height of peaks not associated with groups. Also indicated are the numbers of peaks, groups, groups not associated with peaks, and peaks not associated with groups.

If a particle tagged as a peak in the initial conditions ends up in a group, and it is the highest peak to end up in that group, it is plotted as a "x" in Figure 1 at the appropriate group mass and peak height, ν , in units of the standard deviation, σ , of the linear density field. If the particle is not the highest peak to end up in that group, it is plotted as a "+" in Figure 2. There appears to be a correlation between the mass of a group and the height of the peak in the linear density field from which it comes: $2 \times 10^{11} M_\odot$ groups come from 0 to 1σ peaks while $2 \times 10^{14} M_\odot$ groups come from 3 to 4σ peaks. However, the converse correlation is very weak: although the highest peaks in the initial density field end up in large groups, small peaks can end up in any size group. Furthermore, there are some peaks that do not end up in a group at all. This is illustrated by the line along the

vertical axis, which shows the differential distribution in peak height of peaks that do not end up in groups. Of the ~ 18000 peaks identified in the initial density field with a smoothing of 0.55 Mpc, ~ 4000 never end up in a group, including a few that are greater than 3σ . For the peaks in the density smoothed at 0.88 Mpc the situation is better, with only about 10% of the peaks not ending up in a group; however, there are still a few peaks above 3σ that do not end up in a group.

The line along the horizontal axis shows that all is also not well with the group size to peak correlation. It plots the cumulative distribution in group mass of those groups that have no peak particle in them. For peaks smoothed on a 0.55 Mpc scale, over 1/3 of the groups have no peak associated with them. For the 0.88 Mpc smoothing, over 2/3 of the groups are not associated

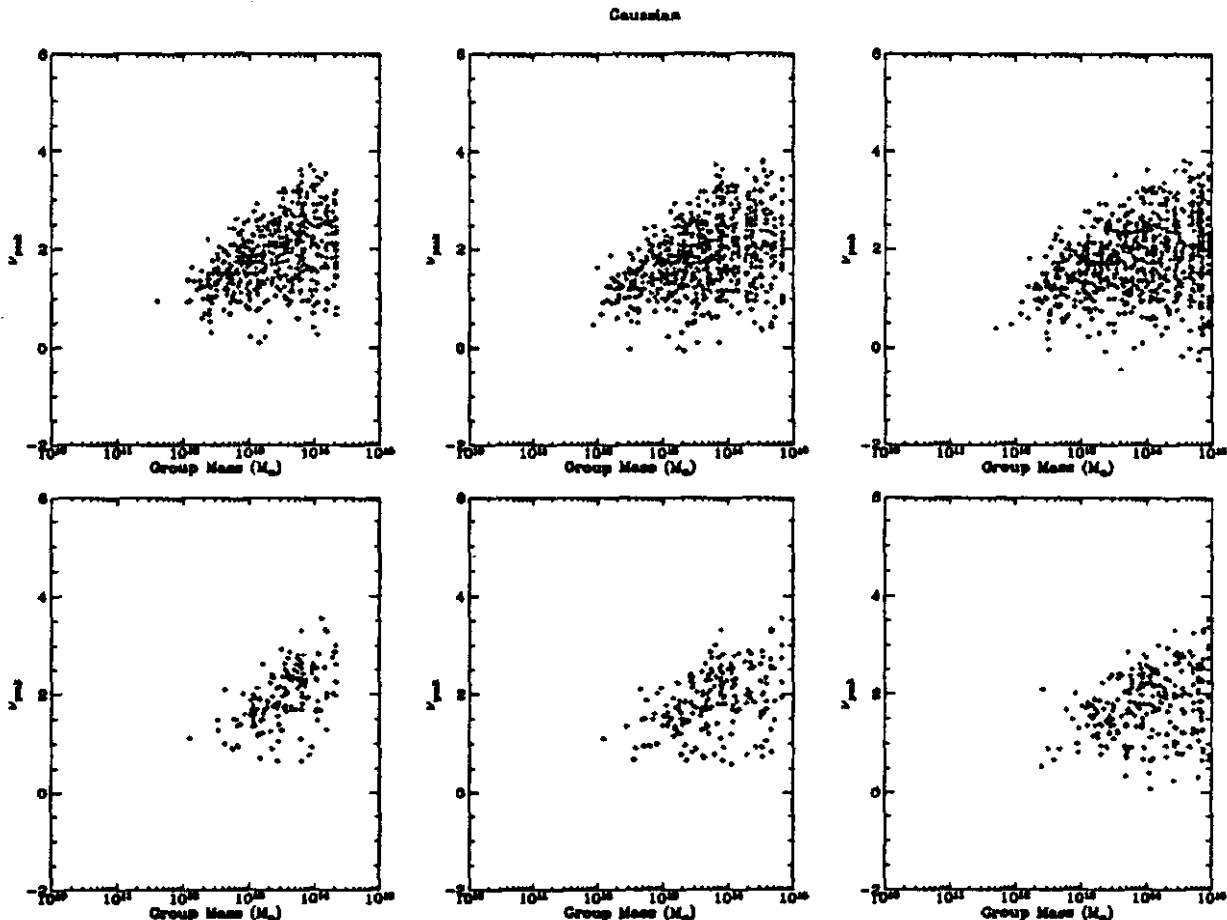


Figure 2. Same as Figure 1 except that peaks associated with a group other than the highest peak in the group are indicated with a “+”.

with a peak in the linear density field. The groups without peaks can be as large as $3 \times 10^{12} M_{\odot}$ and contain over 100 particles.

These plots suggest that using peaks to follow the distribution of galaxy objects is a very poor strategy. If we look at peaks from which cluster size groups form ($\nu = 4\sigma$ and above), then most of those peaks do end up in cluster size objects, but if we look at peaks from which galaxy size objects form ($\nu \approx 2\sigma$), then these peaks have about an equal chance of either ending up in a galaxy size group, or merging with a larger peak to become part of a much larger group.

Perhaps there is another filter that does a better job of finding the peaks in the linear density field that are likely to collapse into groups; we have examined several possibilities. In comparing different filters, we try to match the filter scales by having comparable filter masses. This mass is determined by integrating the background density under the filter function.

In view of the merging problem described above, one promising filter is the sharp k space filter, which is the

Heaviside unit function in k . A cutoff below a scale k_c produces a smoothing function $[k_c^3/(6\pi^2)]W(k_c r)$ where

$$W(x) \equiv \frac{3(\sin x - x \cos x)}{x^3}. \quad (1)$$

Since this function has negative sidelobes, one expects that this filter will tend to pick out isolated peaks, which would be less likely to merge. The mass scale of this filter, given a $R_k \equiv 2\pi/k_c$, is determined by the integral of $W(k_c r)$ over all space giving

$$M_k = \frac{3}{4\pi} R_k^3 \rho_b. \quad (2)$$

Using this formula, the filtering radii are 2.29 Mpc and 3.64 Mpc for $2 \times 10^{11} M_{\odot}$ and $8 \times 10^{11} M_{\odot}$, respectively. The results for these filters are very similar to those plotted in Figures 1 and 2, and show that the sharp k space filter does not do any better than the Gaussian filter and that the correlation between peak height and group mass is even weaker. There seem to be just as many, if not more, peaks that end up merging with larger peaks,

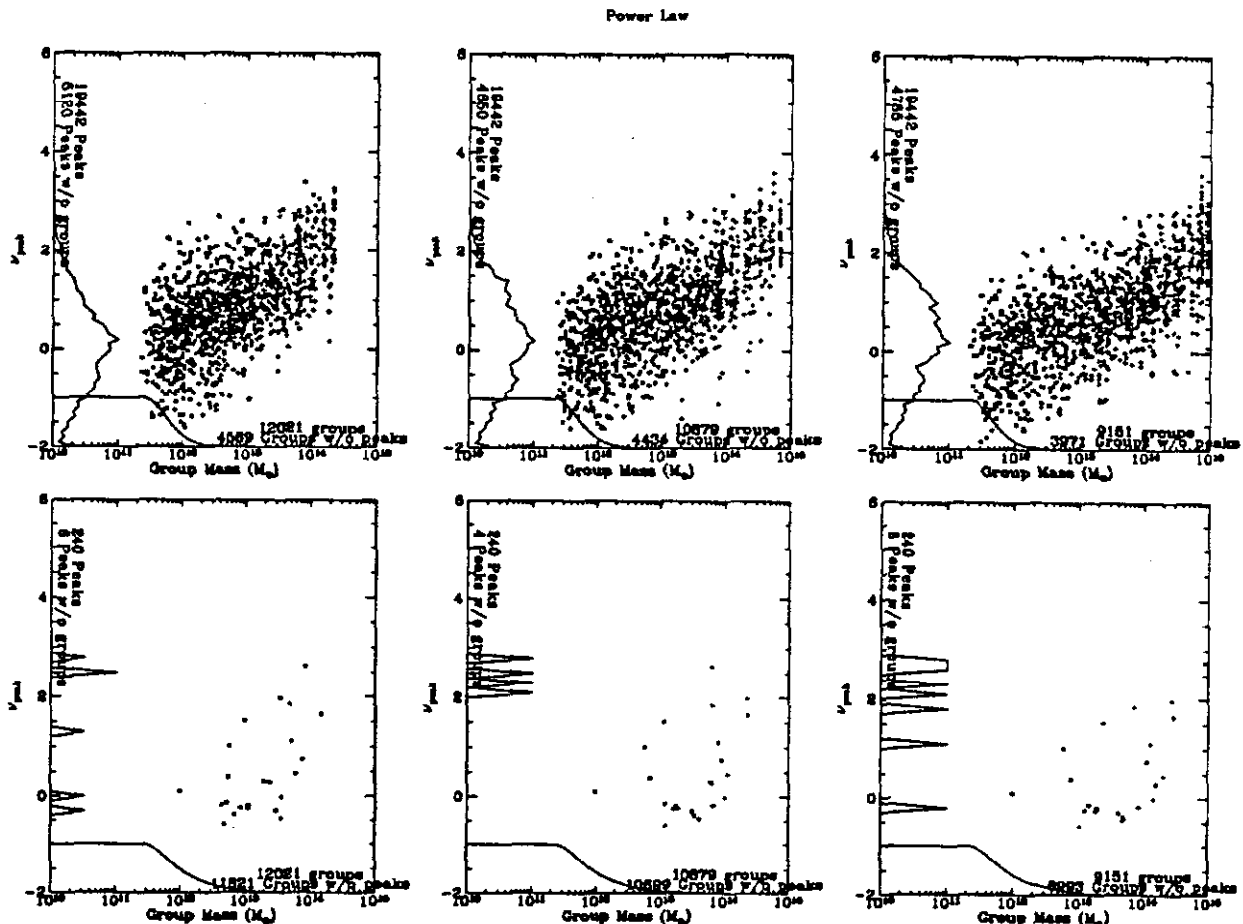


Figure 3. Same as Figure 1, but with a power law filter in k space. The top row is for a power law index of -1 , and the bottom row is for a power law index of -2 . The highest peak associated with a group is plotted with a “ \times ”, and other peaks associated with groups are plotted as “ $+$ ”.

and a higher percentage of the peaks found do not end up in a group. There is also no significant change in the number of groups that have no peak associated with them.

Another popular filter is the top hat filter. Here, the real space representation looks like the k space representation of the sharp k filter, and the k space representation is the function $W(k)$ defined above. The results for this filter with R_{tophat} chosen to match the filter mass scales of Figure 1 were examined. There appears to be no significant difference from the results for a sharp k filter. The only difference of note is that, because the top hat filtered field has more peaks than the sharp k filtered field, there are correspondingly fewer groups that have no peak associated with them. However, there are correspondingly more peaks without groups.

We have also looked at power law filters, that is, $W(k) \propto k^n$. Here there is no simple function describing the real space smoothing function; therefore, there is no easy way to determine a filtering mass scale. We have

chosen two power law indices, $n = -1$ and $n = -2$. The first index is somewhat arbitrary, but the second corresponds to finding peaks in the unsmoothed potential field. The results for these are shown in Figure 3. They are considerably worse than the previous results. The $n = -2$ filter in particular seems to have almost no correlation between group mass and peak height, and despite there being relatively few peaks, there are some quite high peaks that do not end up in a group.

Given a linear potential field, Φ , there are three linearly independent scalars that can be extracted from its second derivatives, constructed from the eigenvalues of the shear tensor, $\zeta_{ij} = \nabla_i \nabla_j \Phi$. The density field is related to the sum of these eigenvalues (trace of ζ_{ij}) from Poisson’s equation:

$$\nabla^2 \Phi = \text{Tr}[\zeta_{ij}] = 4\pi G\rho. \quad (3)$$

If the power spectrum is falling rapidly with k , we would expect the first collapses to occur where the maximum eigenvalue is largest, since the collapse time is primarily dependent on the largest eigenvalue (Zel’dovich 1970).

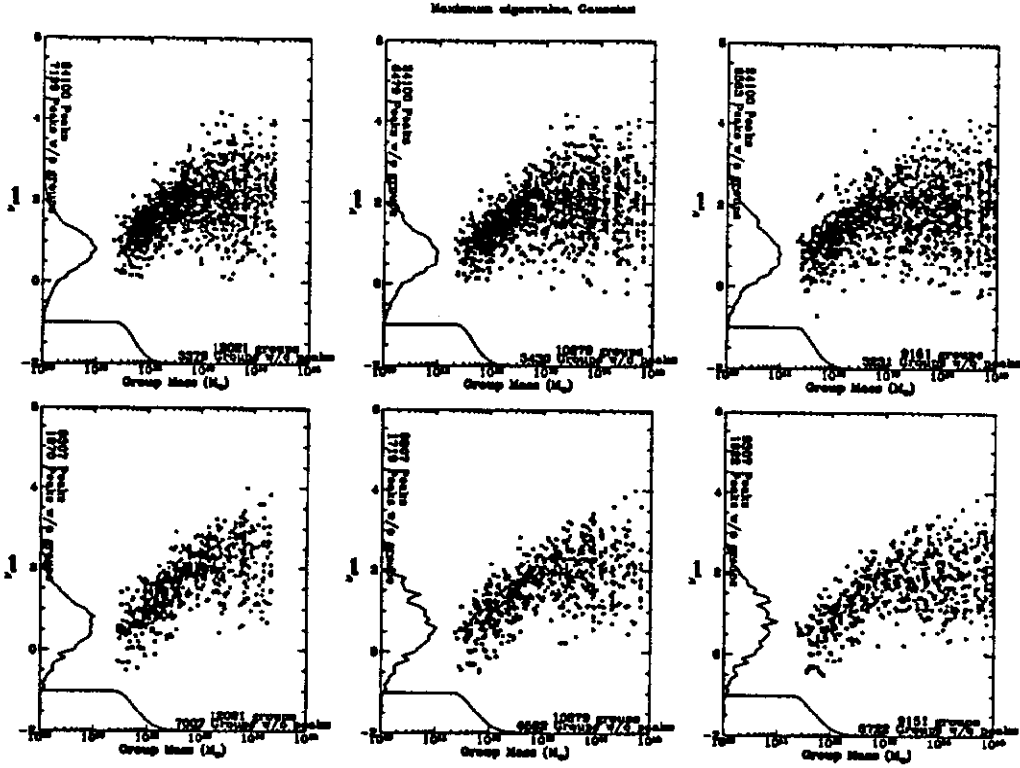


Figure 4. Same as Figure 3, but the peaks are taken from the field of maximum eigenvalues of the shear tensor associated with the density field. The upper row is for a filter length of $R_f = 0.55$ Mpc, while the lower row is for $R_f = 0.88$ Mpc.

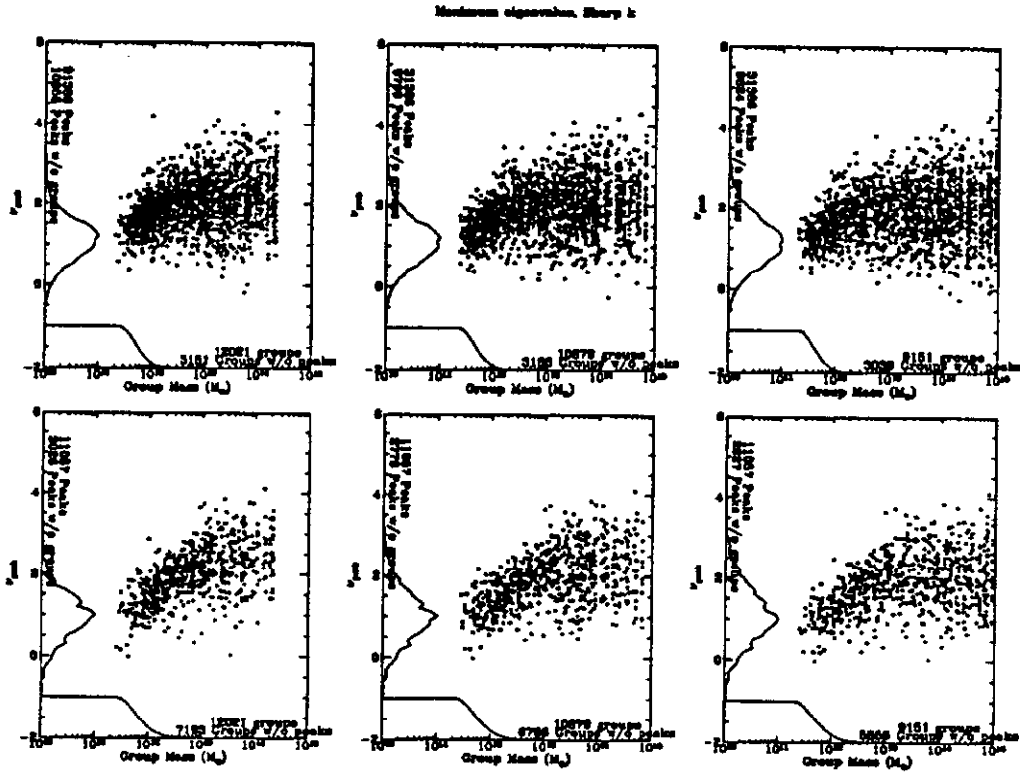


Figure 5. Same as Figure 4, but with a sharp k filter. The top row is for a filter length of $R_k = 2.29$ Mpc, and the bottom row is for $R_k = 3.64$ Mpc.

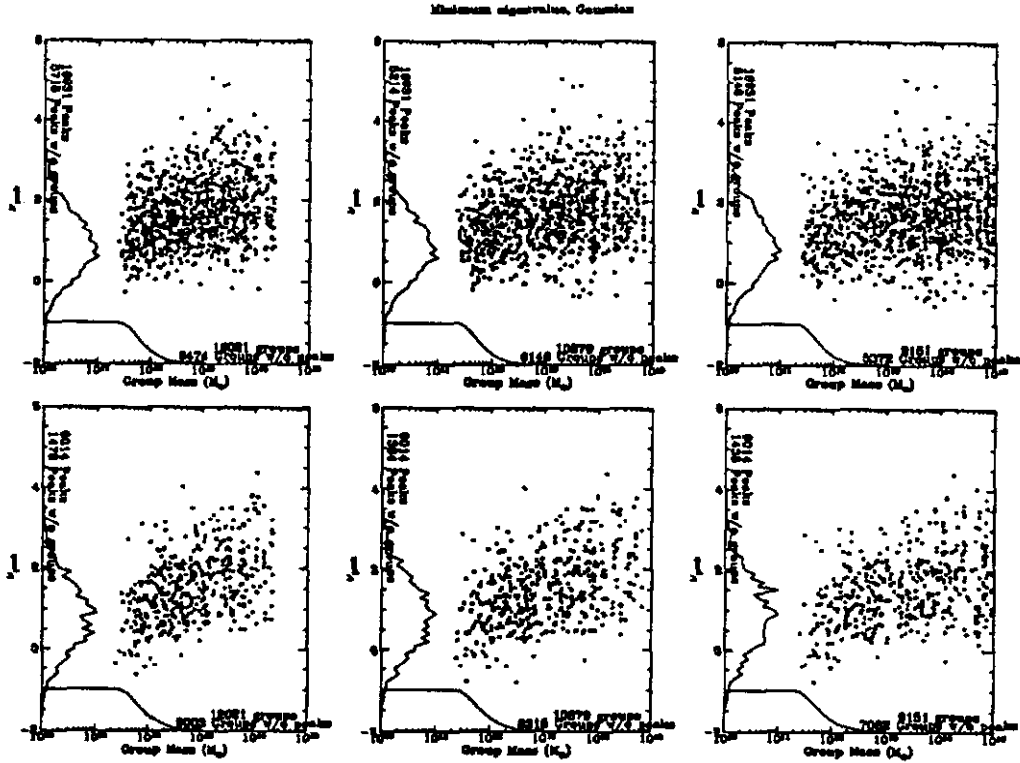


Figure 6. Same as Figure 4, but the peaks are taken from the field of minimum eigenvalues of the shear tensor. The top row is for a filter length of $R_f = 0.55$ Mpc, and the bottom row is for $R_f = 0.88$ Mpc.

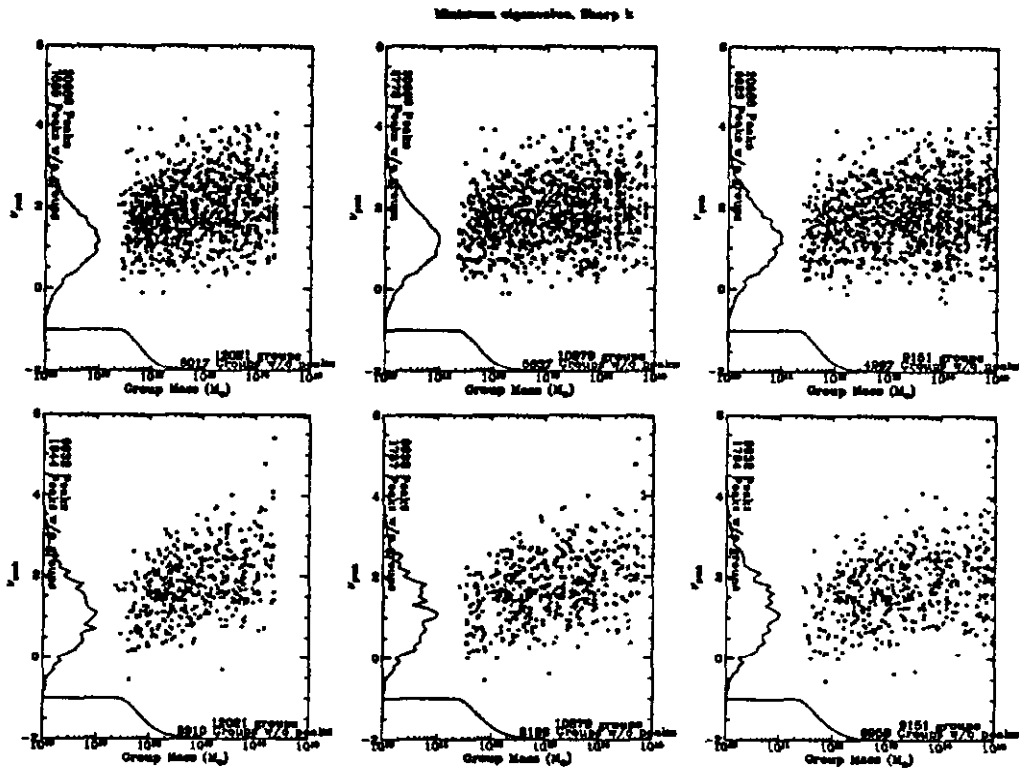


Figure 7. Same as Figure 6, but with a sharp k filter. The top row is for a filter length of $R_k = 2.29$ Mpc, and the bottom row is for $R_k = 3.64$ Mpc.

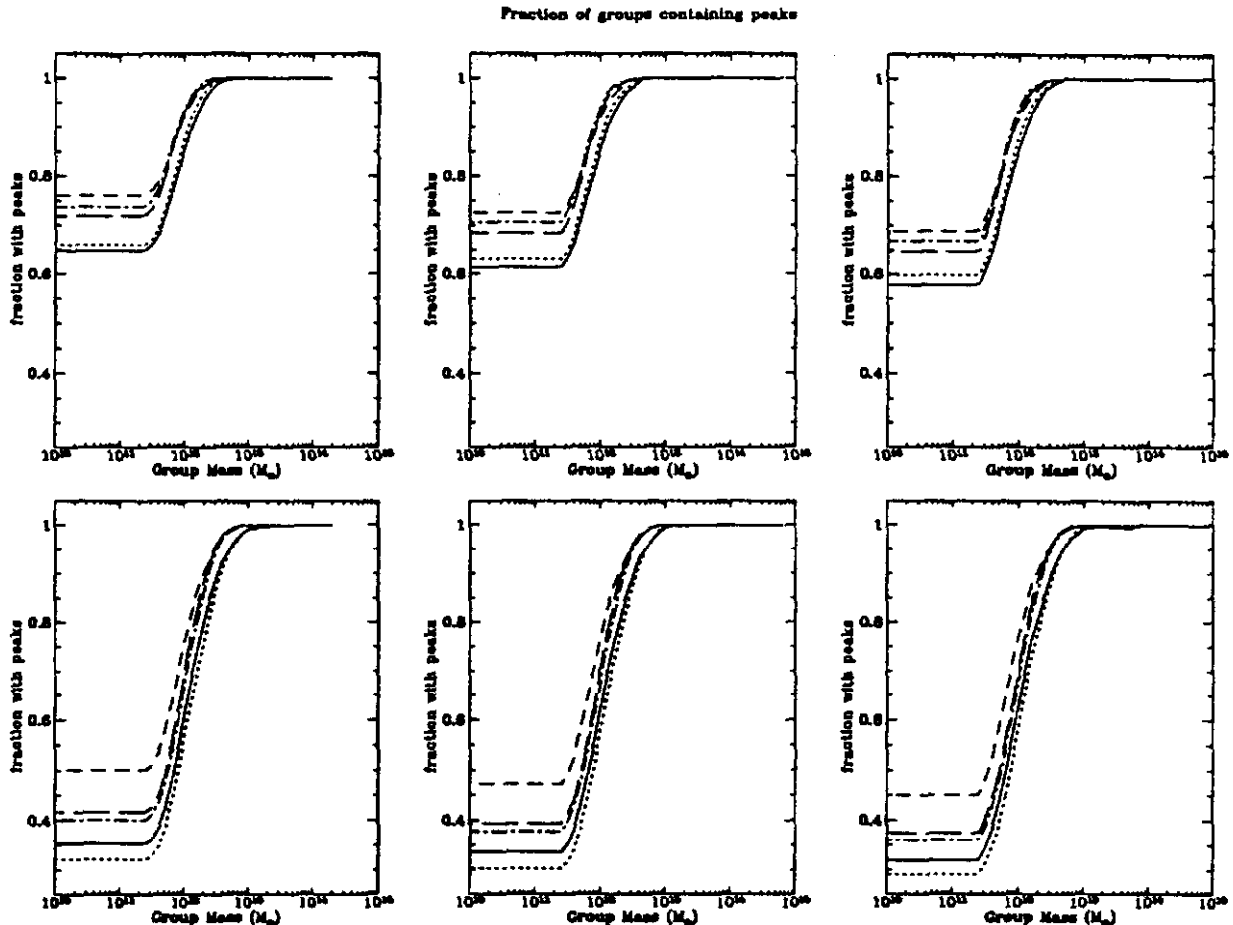


Figure 8. The fraction of groups above a given mass that contain peak particles is plotted against mass. The top row is for filtering on a mass scale of $\sim 2 \times 10^{11} M_{\odot}$, and the bottom row is for filtering on a mass scale of $\sim 8 \times 10^{11} M_{\odot}$. The solid, dotted, and dashed lines are for Gaussian, sharp k , and top hat filtering of the density field, respectively. The long dashed and dot dashed curves are for peaks in the maximum eigenvalue field of the shear tensor associated with the density smoothed with a Gaussian and sharp k filter, respectively.

To study this, we have smoothed the initial density field on a given scale, calculated the shear tensor in k space

$$\zeta_{ij}(k) = \frac{k_i k_j 4\pi G \rho(k)}{k^2}, \quad (4)$$

and transformed to real space to find the eigenvalues. The results for Gaussian smoothed densities and sharp k smoothed densities are shown in Figures 4 and 5, respectively. The results are not significantly better or worse than those obtained directly from the density field.

The other linearly independent quantity to check is the minimum eigenvalue. Results for peaks in the minimum eigenvalue for Gaussian and sharp k space filters are shown in Figures 6 and 7. Here, the correlations between peaks in the field and groups are significantly worse than either the density or the maximum eigenvalue. There is only the slightest trend of increasing peak height with increasing group size, and in every case over half the groups have no peak associated with them.

To make a more general comparison between the above methods for determining the sites of galaxy formation, in Figure 8 we plot the fraction of groups of a given mass or above that contain peaks as a function of group mass for most of the methods described above. Note again, that the methods shown perform almost equally well at finding the peaks that will collapse into groups. With a filter mass of $2 \times 10^{11} M_{\odot}$ about 1/3 of the groups are not found, and with a filter mass of $8 \times 10^{11} M_{\odot}$ over 1/2 the groups are not found. Also, the groups without peaks are not the smallest groups; over one half of them are above $\sim 6 \times 10^{11} M_{\odot}$ for the $2 \times 10^{11} M_{\odot}$ smoothing.

Clearly there is not a good correspondence between peaks in the initial density field and the collapsed groups, but this does not rule out the possibility that the two populations will resemble each other in a statistical sense. To discover if this is the case, we have plotted in Figure 9 the correlation function of the peaks found

Correlations of peaks

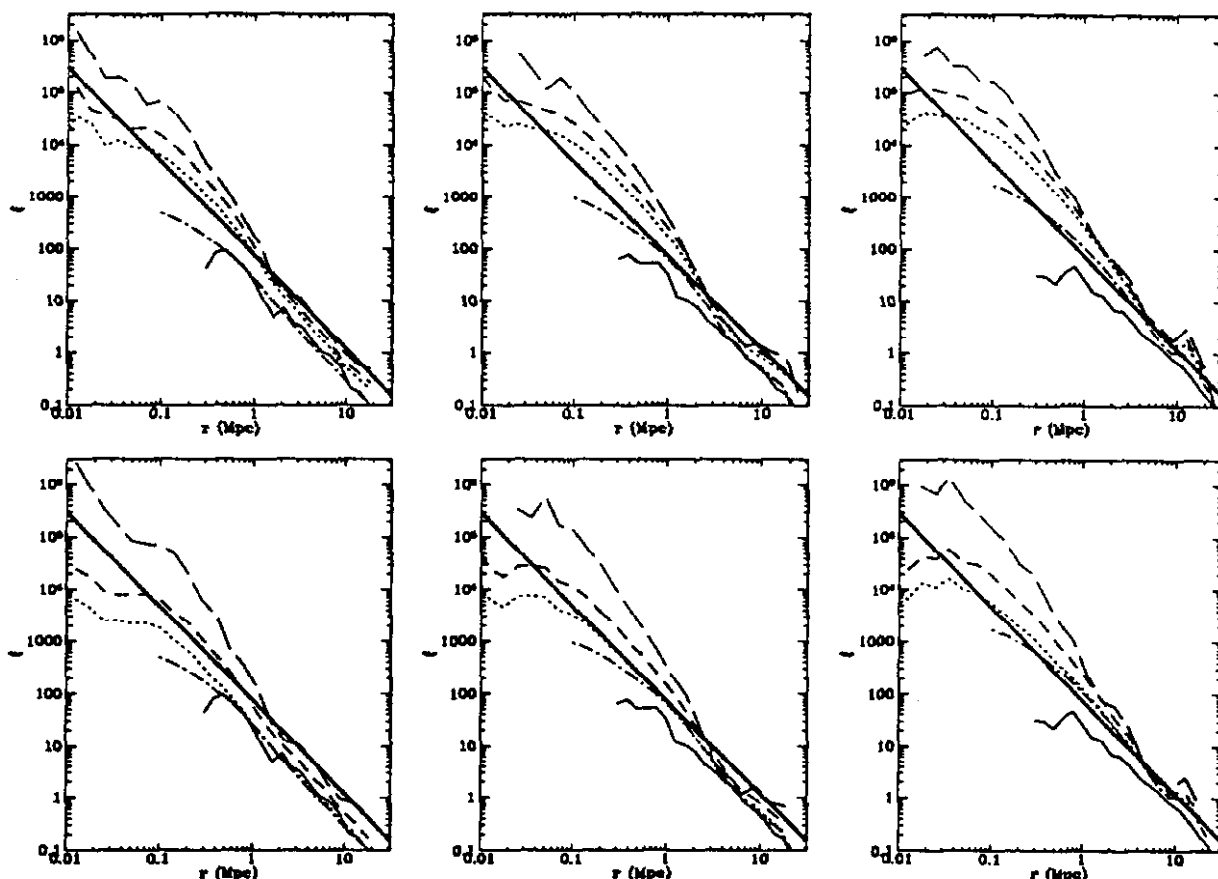


Figure 9. The log of the correlation function is plotted against the log of the separation of the centers for groups, peaks, and mass. The peaks were taken from the Gaussian filtered linear density field. The top row is for a filter length of $R_f = 0.55$ Mpc and the bottom row is for $R_f = 0.88$ Mpc. The straight solid line is a power law with index -1.8 with the observed amplitude ($h = 0.5$). The other solid line is the correlation of the groups. The long dashed, short dashed, and dotted lines are the correlation of peaks with a threshold height chosen so that their number density corresponds to that of L_* , $L_*/10$, and $L_*/100$ galaxies, respectively. The dot dashed line is the correlation of the mass.

with a Gaussian filter on both mass scales, as well as for the mass and for the groups. Here, we have chosen to take only those peaks whose height is above a given threshold, ν_{th} , where ν_{th} is chosen so that the peak number density would match a given galaxy density. Using the luminosity function found by Loveday *et al.* (1992), the observed number densities of $L_*/100$, $L_*/10$, and L_* galaxies correspond to ν_{th} of 1.8, 2.3, and 3.2 for the smaller filter mass, and 0.0, 1.5, and 2.9 for the larger filter mass. Similarly, we calculate the correlation function of only those groups whose circular velocity at 200 kpc is greater than 250 km s^{-1} , corresponding to L_* and above galaxies.

The naive expectation is that the group correlation function should match the peak correlation function corresponding to L_* galaxies, which is not the case. In fact, the group correlation function is anti-biased with respect to the mass correlation function at all but the

earliest times. This anti-biasing is mostly due to over-merging, *i.e.* the large clusters are only identified as one group instead of many groups, and is discussed in much greater detail in Gelb (1992). Although the amplitude of the group correlation function is smaller than that observed, it has the correct power law form and slope. When the galaxies are reinserted into the clusters, as also described in Gelb (1992), the amplitude of the group correlation function can be increased while retaining the correct power law form.

The peaks are more correlated than the mass so they are biased with respect to the dark matter. As expected, the peaks corresponding to more luminous galaxies are more biased than those that correspond to less luminous galaxies, and the degree of biasing gets smaller at larger expansion factors. At scales greater than ~ 2 Mpc the correlation function of the L_* peaks even closely resembles the observed galaxy correlation function. Within

Pairwise velocity dispersions

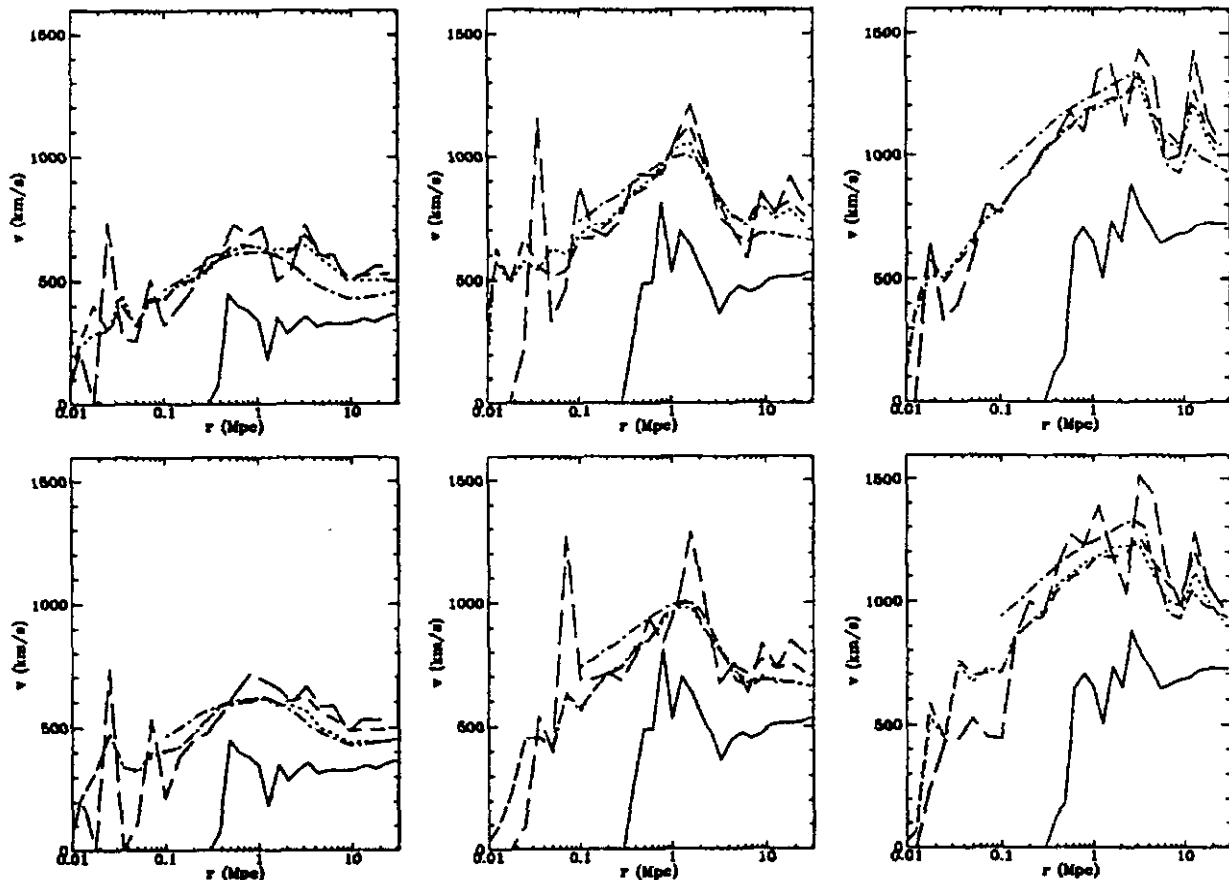


Figure 10. The one dimensional velocity dispersion along the line of separation, σ_{\parallel} , is plotted against the log of the separation. The solid line is for the groups. The long dashed, short dashed, and dotted lines are for the peaks as in Figure 9, and the dot dashed line is for the mass.

~ 2 Mpc, however, the peak correlation function becomes much steeper than the observed correlation function. At ~ 100 kpc, the correlation amplitude of the L -peaks is over 10 times too large.

Another statistic is the one dimensional pairwise velocity dispersion along lines of separation. We plot these for the same populations as Figure 9 in Figure 10. Here, the peak velocity dispersions follow those of the mass quite closely, and do not show the “velocity bias” that is seen in the groups (Carlberg *et al.* 1990; Bertschinger and Gelb, 1991). If the large clusters are broken up, as was done for the correlation function, then the velocity dispersions of the resulting groups can be increased so that they also match the mass (Gelb 1992). Even with a velocity bias, only at an expansion factor of 0.5 is the group velocity dispersion low enough to match the observed dispersion of $\sim 300 \pm 50 \text{ km s}^{-1}$ (Davis and Peebles, 1983).

4 DISCUSSION

The results presented above contradict the conclusion of FWDE that groups that form are closely related to peaks in the smoothed linear density field. The biggest difference between our work and theirs is the size of our simulation: 100 Mpc compared with 14 Mpc. However, there are other small differences. (i) The mass of the particles in the simulation discussed here is $2.324 \times 10^{10} M_{\odot}$, a factor of 4 larger than that used in the FWDE results. The softening parameter is also correspondingly larger. (ii) FWDE do their analysis for epochs corresponding to a relatively high bias. They looked at biases of 7, 4, and 2, compared to our highest bias of 2. (iii) They use a friends-of-friends group finding algorithm instead of the DENMAX routine used here. The advantage of the DENMAX algorithm over friends-of-friends is its ability to break up large dense clusters into subgroups while still being able to detect smaller, less dense halos in the field. This is discussed in detail in Gelb (1992). (iv) FWDE only consider peaks in the

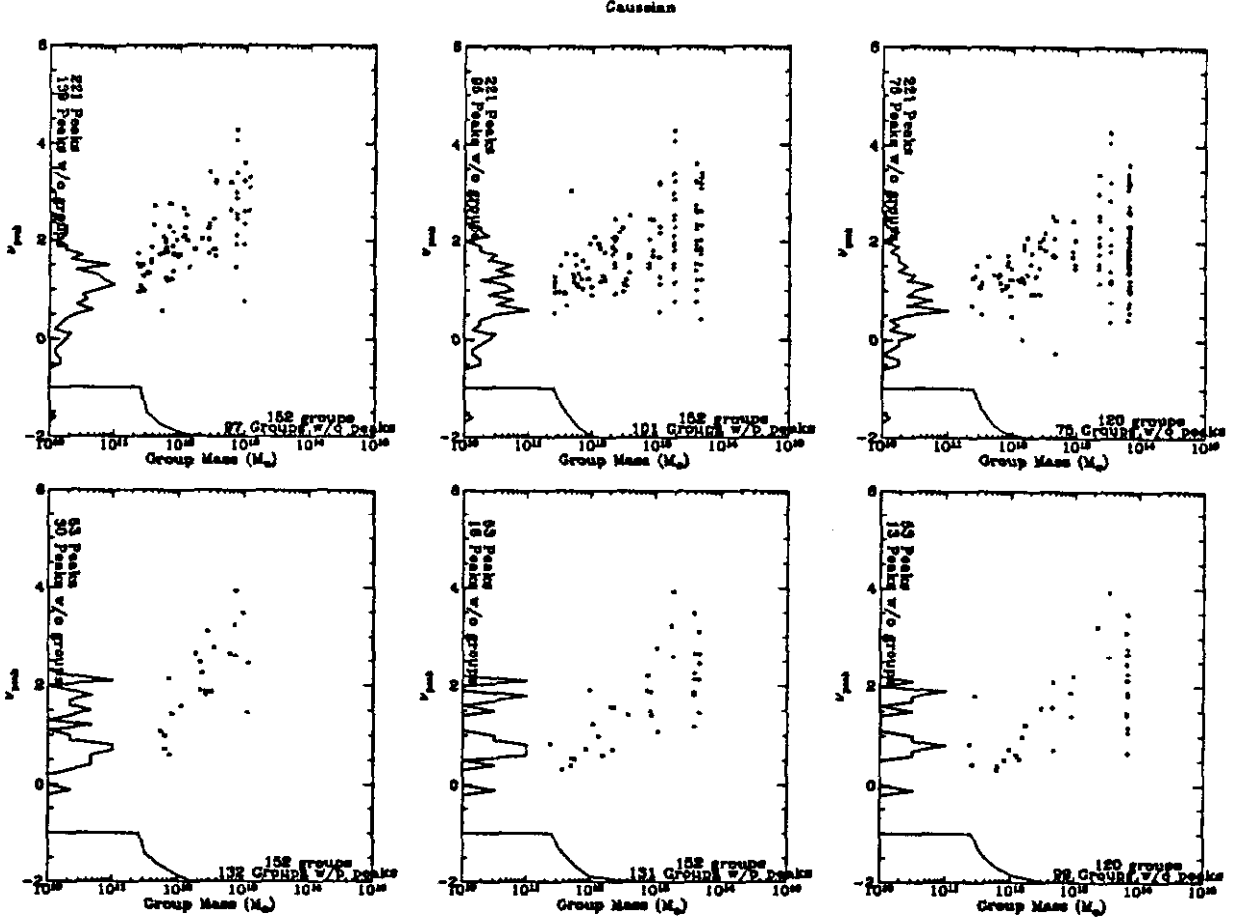


Figure 11. The same as Figure 3, but for the 14 Mpc simulations, and with expansion factors of $\alpha = 0.25, 0.5,$ and 0.7 . All peaks from three simulations are plotted.

linear density field with heights above a threshold of 1σ , while we consider peaks of all heights.

In order to help determine which of these differences leads to the different conclusions, we have created small simulations with the same mass resolution as the large simulation described above, but with a box size of only 14 Mpc as in FWDE. Such a simulation contained only 8000 particles. We then found peaks in the initial density field as before, and used the friends-of-friends algorithm with a linking parameter of 0.2 times the mean interparticle separation to find the groups. We also looked at an earlier epoch of $\alpha = 0.25$ corresponding to $b = 4.0$. In this way we can isolate the one aspect of our simulations that is inferior to those of FWDE: the larger particle mass. In order to have a reasonable number of groups, we simulated three realizations of the 14 Mpc box. The results of this exercise are presented in Figure 11, where the left panels are for $\alpha = 0.25$, the middle panels are for $\alpha = 0.5$, and the right panels are for $\alpha = 0.7$. With the exceptions that FWDE combine simulations with several different Ω in an attempt to model

the effects of large scale power, and that they only consider peaks above 1σ , the left panels of Figure 11 should be directly comparable with the middle panels of Figure 13 in FWDE. Likewise, the middle panels of Figure 11 should be compared with the right panels in Figure 13 of FWDE.

The results of our small simulations compare reasonably well with those of FWDE. The biggest difference is that FWDE have quite a few groups between $1 \times 10^{11} M_{\odot}$ and $3 \times 10^{11} M_{\odot}$, which seem to be too small for our simulations to resolve. Otherwise our results are remarkably similar. For the larger smoothing, the largest peaks that do not end up in a group are just above 2σ , and many such peaks are below 1σ . For the smaller smoothing, we have one or two peaks above 2.5σ that do not collapse whereas FWDE have none. However, the same general trend of peak height and group size is observed, and there are a similar number of mergers. Therefore, it appears that the resolution is not affecting our results at either smoothing scale.

The FWDE conclusion about the correspondence of

peaks and groups is really only supported at the very high biases of 4 and 7. At the more reasonable bias of 2, their results show the same problems we have presented above, namely, (i) smaller peaks can end up in any size group by merging with a higher peak, (ii) there are a few (albeit not many) high peaks that do not end up in groups, and (iii) there are many groups of quite high mass that are not associated with any peak.

The first of these problems is the least surprising, since it is one aspect of the "overmerger problem" that arises when trying to match the predictions of CDM to the observations of galaxy clusters. As discussed in FWDE, the groups in clusters merge much too quickly, and if CDM is to be viable, there must be some mechanism preventing the visible parts of galaxies from merging as their dark halos merge. Recent works (Katz and White 1992; Katz, Hernquist, and Weinberg 1992; Evrard *et al.*, in preparation) that include gas dissipation show that this is indeed the case and that several galaxies can exist in a common dark matter envelope. The question that naturally arises is whether the peaks are a better indicator of the sites of galaxy formation than identifying groups in a dissipationless simulation. If this were true, it would be a serious blow to the CDM model. The peak correlation function can be made sufficiently strong at 10.8 Mpc to match the observed correlation length but it becomes much too steep at scales less than 2 Mpc. At these small scales the overmerger problem has the greatest effect on the correlation function. In addition, since the velocities of the peaks are similar to the velocities of the dark matter, only at $b \gtrsim 2$ are the peak velocities low enough to match the observed values. Given the generally poor correspondence between peaks and groups outside of the clusters, however, there is no compelling reason to believe that the peaks miraculously identify the sites of galaxy formation within the clusters.

Indeed, if the overmerging is accounted for by using an artificial but reasonable mechanism to break the largest halos into galaxy size objects (White *et al.* 1987a, Gelb 1992), then the correlation function can be increased enough to match the observed value at 10.8 Mpc while retaining the proper power law slope. When this is done the pairwise velocity dispersions, which are lower than those for the dark matter, increase significantly and more closely resemble those of the peaks. However, boosting the correlation function by breaking up the largest halos may require more than the observed number of galaxies (Gelb 1992). In contrast, the peak correlation function can be made sufficiently strong at 10.8 Mpc using the correct numbers of galaxies. Finally, it should be noted that in the dissipational simulation of Katz, Hernquist, and Weinberg (1992), where the galaxies are identified as cold condensed regions of gas, the galaxy correlation function follows a power law from

35 kpc to 10 Mpc and has the correct enhancement over that of the dark matter to match the observed correlation amplitude.

The second problem is more unexpected, but it shows that just having a high peak in the density field does not imply the formation of a group from that material. The eventual fate of such peaks is unclear.

The third problem has the most damning implications for the high peak model. Even in the FWDE $b = 2$ high resolution simulations, there are groups above $10^{12} M_{\odot}$, composed of hundreds of particles, but associated with no peak. This is a problem that is exacerbated in the larger simulations as can be seen from the median mass of the groups without peaks. The median mass of groups that have no peak can be read off the bottom line of the figures. For the small simulations and the smaller filter, this median mass is between $3 \times 10^{11} M_{\odot}$ and $4 \times 10^{11} M_{\odot}$. For the large simulation with a Gaussian filter of mass $2 \times 10^{11} M_{\odot}$ this mass is $6 \times 10^{11} M_{\odot}$, $5.5 \times 10^{11} M_{\odot}$, and $5 \times 10^{11} M_{\odot}$ for $\alpha = 0.5, 0.7,$ and 1.0 , respectively. This mass is $7.5 \times 10^{11} M_{\odot}$, $6 \times 10^{11} M_{\odot}$, and $5.5 \times 10^{11} M_{\odot}$ for a filter mass of $8 \times 10^{11} M_{\odot}$.

The comparison with FWDE also questions the wisdom of just considering peaks above a threshold ν_{th} . In the linear theory of BBKS, the biasing of the peaks with respect to the density depends upon ν_{th} (or a selection function) and roughly scales as $b \approx \nu_{th}$ in the high peak limit. As mentioned above, another advantage in considering peaks above a certain threshold is that it matches the correct number density of galaxies by construction. However, making such a cut in ν_{th} throws out many of the groups. To investigate this in detail we examined the groups at $\alpha = 0.5$ whose circular velocity at 200 kpc is greater than 250 km s^{-1} , corresponding to L_* and above galaxies. We checked these groups to see if they contained any peaks. To correctly match the number of galaxies this meant choosing $\nu_{th} = 2.95$ for $R_s = 0.55$ Mpc and $\nu_{th} = 2.50$ for $R_s = 0.88$ Mpc. Of the 737 groups, 53% did not contain a peak for $R_s = 0.55$ Mpc and 48% for $R_s = 0.88$ Mpc. So using the standard technique of considering peaks above a certain threshold just exacerbates the lack of correspondence between peaks and groups.

The correlation function and the pairwise velocity distribution give us a clue about which groups are being missed by the peaks. The correlation function is steeper than that of the mass, and the velocity dispersion is comparable to the mass velocity dispersion. This indicates that many of the peaks are found in large clusters, and the groups that are being missed are those in the field (see also Gelb 1992). This is to be expected, as the probability of a peak being above a given threshold is much greater in a cluster where there is a general density enhancement.

The difference in the median mass of groups with no

corresponding peak between the large and small simulations hints that fluctuations on larger scales are affecting the way in which groups form, possibly through their tidal fields (Quinn and Binney 1992). Peaks, being local phenomena, would have no mechanism for determining tidal fields over large distances. Since peaks are overdense and, therefore gravitationally unstable regions, they must collapse to form groups in the absence of any external forces. Large scale tidal fields could produce an external shearing force that may prevent some peaks from collapsing and forming groups. Similarly, convergent flows might allow regions to become locally gravitationally unstable and collapse even though the regions were unassociated with any local density peak.

The above results have serious implications for the study of galaxy formation. Since peaks are not good indicators of the sites of galaxy formation, one should be cautious when inferring galaxy properties from the properties of peaks (*e.g.* BBKS, Heavens and Peacock 1988, Quinn and Binney 1992). The same caution should be applied when using peaks as the initial conditions for simulations of galaxy formation (*e.g.* Dubinski and Carlberg 1991). Moreover, since it appears that large scale forces affect the evolution of local density peaks, volumes that are much larger than galaxy scales are probably necessary to simulate individual galaxy formation properly. In fact, it was while trying to simulate the formation of individual galaxies using peaks in the initial density field as initial conditions (set up using the method of Binney and Quinn (1991)) that we first realized that peaks did not correspond very well with the sites of galaxy formation. The lack of correspondence became much worse as we made our volume larger. It was these simulations that originally motivated the current work. Finally, although this work does not address cluster formation, it also brings into question studies that assume that clusters form at peaks, something that will have to be studied in future simulations.

The above results also have serious implications for the use of peak tracers or peak-background rejection methods in large scale structure simulations. Since the peaks do not succeed in determining the sites of galaxy formation, then in the absence of any other criteria for relating the density field to the galaxy distribution, any large scale structure simulation must have enough resolution to follow the formation of galaxy halos. To simulate a volume the size of the Stromlo-APM redshift survey (Loveday *et al.*, 1992), this would require $\sim 2 \times 10^9$ particles of $2 \times 10^{10} M_{\odot}$. This is clearly impossible unless there is a several order of magnitude increase in computing technology.

5 CONCLUSIONS

Our main conclusion is that peaks in the linear density field are not good indicators of the sites of galaxy

formation as determined by the dissipationless collapse of halos. It is possible that processes not considered, such as gas-dynamical feedback, could considerably alter this result by suppressing the formation of galaxies in the field in the same manner that peak selection does. However, it would seem quite a coincidence if those processes conspired to give the same effect as the statistical process of selecting high peaks. One process considered that could be gas-dynamical in nature was the solution of the overmerging problem by allowing galaxies to remain distinct after their halos have merged. In this case some statistical properties of the galaxies are more similar to those of the peaks than to those of the halos, so such a conspiracy between gas-dynamics and the statistics of peaks is not inconceivable. Another caveat is that we have only investigated simulations with a CDM initial power spectrum, and the results for other initial power spectra could be different—it is likely, however, that the above results would hold for any power spectrum that is similar to CDM in the sense that it has significant power over a large range of length scales.

It is quite unfortunate that the results presented here appear to invalidate the usual method for determining the galaxy distribution from the mass density in large scale structure simulations. This leaves the choice of either going back to the assumption that the galaxy distribution is an unbiased sample of the mass distribution, or investigating a new method for determining sites of galaxy formation. The first option is unpleasant because it means that the comparison of existing CDM simulations with existing observations almost conclusively rules out the theory. As we have been exhaustive in investigating linear criteria, the second option will almost certainly entail the investigation of nonlinear effects, multiple filters, or dynamical considerations, which will preclude the use of the formalism of BBKS, and make the ability to estimate galaxy densities from mass densities on larger scales quite difficult.

6 ACKNOWLEDGMENTS

The supercomputing portion of this research was conducted using the Cornell National Supercomputer Facility, a resource of the Center for Theory and Simulation in Science and Engineering at Cornell University, which receives major funding from the National Science Foundation and IBM Corporation, with additional support from New York State and members of its Corporate Research Institute. Thomas Quinn was supported by SERC grants LMDR-GRH11297 and HKDB-GRH32711. Neal Katz acknowledges the award of a Hubble Fellowship. James M. Gelb was supported in part by NSF grant AST90-01762 (at M.I.T.), by the DOE (at Fermilab), and by NASA grant NAGW-2381 (at Fermilab).

It is a pleasure to thank Cedric Lacy, James Binney, George Efstathiou, and Eric Linder for useful comments and discussions. We wish to give a special thanks to Ed Bertschinger for comments and collaboration with the development of the N-body code and DENMAX.

7 REFERENCES

- Bardeen, J.M., Bond, J.R., Kaiser, N., and Szalay, A.S. 1986. *Astrophys. J.*, **304**, 15.
- Bertschinger, E. and Gelb, J.M. 1991. *Computers in Physics*, **5**, 164.
- Binney, J. and Quinn, T. R. 1991. *Mon. Not. R. astr. Soc.*, **249**, 678.
- Carlberg, R.G., Couchman, H.M.P., and Thomas, P. 1990. *Astrophys. J. Lett.*, **352**, L29.
- Couchman, H.M.P. 1990. *Astrophys. J. Lett.*, **368**, L23.
- Dalton, G. B., Efstathiou, G., Maddox, S. J., and Sutherland, W. J. 1992. *Astrophys. J. Lett.*, **390**, L1.
- Davis, M., Efstathiou, G., Frenk, C.S., and White, S.D.M. 1985. *Astrophys. J.*, **292**, 371.
- Davis, M. and Peebles, P.J.E. 1983. *Astrophys. J.*, **267**, 465.
- Dekel, A. and Silk, J. 1986. *Astrophys. J.*, **303**, 39.
- Dubinski, J. and Carlberg, R.G. 1991. *Astrophys. J.*, **378**, 496.
- Frenk, C.S., White, S.D.M., Davis, M., and Efstathiou, G. 1988. *Astrophys. J.*, **327**, 507.
- Frenk, C.S., White, S.D.M., Efstathiou, G., and Davis, M. 1990. *Astrophys. J.*, **351**, 10.
- Gelb, J.M. 1992. M.I.T. Ph.D. thesis.
- Heavens, A. and Peacock, J. 1988. *Mon. Not. R. astr. Soc.*, **232**, 339.
- Kaiser, N. 1984. *Astrophys. J. Lett.*, **284**, L9.
- Katz, N., Hernquist, L., and Weinberg, D.H. 1992. *Astrophys. J. Lett.*, in press
- Katz, N. and White, S.D.M. 1992. *Astrophys. J.*, submitted
- Loveday, J., Peterson, B.A., Efstathiou, G., and Maddox, S.J. 1992. *Astrophys. J.*, in press.
- Park, C. 1990. *Mon. Not. R. astr. Soc.*, **242**, 59p.
- Park, C. 1991. *Mon. Not. R. astr. Soc.*, **251**, 167.
- Park, C. and Gott, J.R. III 1991. *Mon. Not. R. astr. Soc.*, **249**, 288.
- Quinn, T. and Binney, J. 1992. *Mon. Not. R. astr. Soc.*, **255**, 729.
- Weinberg, D.H. and Gunn, J.E. 1990. *Astrophys. J. Lett.*, **352**, L25.
- White, S.D.M., Davis, M., Efstathiou, G., and Frenk, C.S. 1987a. *Nature*, **330**, 451.
- White, S.D.M., Frenk, C.S., Davis, M., and Efstathiou, G. 1987b. *Astrophys. J.*, **313**, 505.
- Zel'dovich, Ya. B. 1970. *Astron. Astrophys.*, **5**, 84.